

Propagation of scalar waves in dense disordered media exhibiting short- and long-range correlations

Adrien Rohfritsch, Jean-Marc Conoir, Tony Valier-Brasier, Romain Pierrat, Régis Marchiano

▶ **To cite this version:**

Adrien Rohfritsch, Jean-Marc Conoir, Tony Valier-Brasier, Romain Pierrat, Régis Marchiano. Propagation of scalar waves in dense disordered media exhibiting short- and long-range correlations. Physical Review E , 2021, 104 (6), pp.064138. 10.1103/physreve.104.064138 . hal-03813660

HAL Id: hal-03813660
https://hal.science/hal-03813660

Submitted on 13 Oct 2022

HAL is a multi-disciplinary open access archive for the deposit and dissemination of scientific research documents, whether they are published or not. The documents may come from teaching and research institutions in France or abroad, or from public or private research centers.

L'archive ouverte pluridisciplinaire **HAL**, est destinée au dépôt et à la diffusion de documents scientifiques de niveau recherche, publiés ou non, émanant des établissements d'enseignement et de recherche français ou étrangers, des laboratoires publics ou privés.

Propagation of scalar waves in dense disordered media exhibiting short- and long-range correlations

Adrien Rohfritsch,[1] Jean-Marc Conoir,[1] Tony Valier-Brasier,[1] Romain Pierrat,[2] and Régis Marchiano[1]
[1]*Sorbonne Université, CNRS, Institut Jean Le Rond ∂'Alembert, UMR 7190, 4 Place Jussieu, Paris, F-75005, France*
[2]*ESPCI Paris, PSL University, CNRS, Institut Langevin, 1 rue Jussieu, F-75005 Paris, France*

(Received 22 July 2021; accepted 10 December 2021; published 27 December 2021)

Correlated disorder is at the heart of numerous challenging problematics in physics. In this work we focus on the propagation of acoustic coherent waves in two-dimensional dense disordered media exhibiting long- and short-range structural correlations. The media are obtained by inserting elastic cylinders randomly in a stealth hyperuniform medium itself made up of cylinders. The properties of the coherent wave is studied using an original numerical software. In order to understand and discuss the complex physical phenomena occurring in the different media, we also make use of effective media models derived from the quasicrystalline approximation and the theory of Fikioris and Waterman that provides an explicit expression of the effective wave numbers. Our study shows a very good agreement between numerical and homogenization models up to very high concentrations of scatterers. This study shows that media with both short- and long-range correlations are of strong interest to design materials with original properties.

DOI: 10.1103/PhysRevE.104.064138

I. INTRODUCTION

Wave propagation in heterogeneous media made of particles randomly distributed into a host medium has been subject to intense research for more than half a century. Different transport regimes exist, which depend on the size and degree of disorder of the medium [1,2]. For weak disorder, the mean field takes the form of a coherent wave that can be described thanks to multiple scattering theories. In particular, it can be shown that this coherent wave propagates in an effective homogeneous medium with a complex wave number k_{eff} [3,4]. It is well known that the correlations between scatterers strongly impact coherent waves [5–7]. These correlations come into play for understanding, for example, the properties of many various living systems [8,9] or liquid metal [10], and many theoretical studies have been developed with a view to design new materials [11,12].

Existing studies focus on either short-range correlations (SRCs), such as for hard disk systems for instance, or long-range correlations as those that essentially characterize stealth hyperuniform (SHU) materials [13,14]. Nevertheless, no studies address the question of the propagation of scalar waves in media composed of both short- and long-range correlations. In this paper, we focus on the impact of the increase of scatterers size on the coherent waves and we propose two statistical models to capture the complex effects associated with materials exhibiting short- and long-range correlations.

To ensure that the short- and long-range correlations coexist, the idea is to build a new medium by inserting random particles into a SHU medium. The important point is that the considered particles are not pointlike scatterers, they have a finite size and then cannot overlap. It follows that increasing concentration leads to a strengthening of the coupling between the two populations: the SHU particles constrain more and more the random ones, which have less space to fit between the SHU particles. Thus, random particles organize themselves to give a SRC medium. Finally, one gets a nested medium, composed of the SHU and SRC media, exhibiting both short- and long-range correlations.

In the following, our analysis will be based on the properties of the pair-correlation function $h_2(r)$ and the structure factor $S(\mathbf{q})$ [7]. These two quantities are important to describe the correlation effects, first from the point of view of the microstructure of the media [13], but also they enter into the analytical expressions of k_{eff} that lead to a clear physical interpretation of the propagation [15]. Then, the domain of validity of different statistical propagation models providing k_{eff} is studied by comparisons with numerical simulations made with an in-house software, called MuScat [16]. It is based on the exact equations of the multiple scattering theory.

The paper is organized as follows. In Sec. II, the microstructure of the media of interest is exposed that enlightens the specificities of each pattern. In Sec. III the comparison between a first-order statistical model, which does not take correlation effects into account, and numerical results are exposed in order to analyze the propagation of the coherent waves. Section IV is dedicated to the derivation of effective wave numbers and scattering mean-free paths taking into account correlation effects. In Sec. V physical results are discussed.

II. ANALYSIS OF THE MICROSTRUCTURES

In this section, we are interested in the microstructure of the nested medium (SHU + SRC) and the correlations are examined throughout the behavior of the pair-correlation function $h_2(r)$ and the structure factor $S(\mathbf{q})$, where $\mathbf{q}$ is the scattering vector. The structure factor plays an important role

 ©2021 American Physical Society

in the definition and the study of the transparency of SHU media, which are known, as it will be discussed later, to induce almost no loss on propagation of waves at low frequency [17–21]. Let us start by presenting these media in the case where scatterers are of finite size, which induces constraints on the radius of the particles a and the appearance of a cutoff frequency for transparency.

A. Stealth-hyperuniform medium: A correlated disorder that cancels normalized density fluctuations at large wavelength

Stealth hyperuniform media are characterized by the cancellation of normalized density fluctuations at large wavelengths [22,23]. In the Fourier space, this can be described by the structure factor. For N pointlike scatterers, it is given by

$$S(\mathbf{q}) = \frac{1}{N}\left|\sum_{j=1}^{N} e^{i\mathbf{q}.\mathbf{r}_j}\right|^2. \tag{1}$$

The SHU property implies that the structure factor $S_{\mathrm{SHU}}(\mathbf{q})$ verifies [13,24]

$$S_{\mathrm{SHU}}(\mathbf{q} \in \Omega) = 0, \tag{2}$$

where Ω is a domain surrounding (but excluding) the origin. Property (2) implies the transparency of SHU media in the low-frequency limit and for the single scattering regime.

For an infinite medium, Ω is continuous. In the case of a more realistic domain of size L, it is convenient to consider it as an unit cell of a periodic media [25]. Doing so, the domain Ω is discretized.

It is convenient for Ω to choose a square domain of size $2K$ around the origin. Doing so, the discrete wave numbers $\mathbf{q}$ are given by $(n_x, n_y)2\pi/L$, with $-P < (n_x, n_y) < P$, and $P = KL/(2\pi)$. The degree of stealthiness is defined as the ratio between $M(\Omega)$, the number of constraint wave numbers $\mathbf{q} \in \Omega$ and the number of degrees of freedom [$2N$ in the case of a two-dimensional (2D) point pattern] [24,25]:

$$\chi = \frac{M(\Omega)}{2N} \tag{3}$$

leading to the following expression for K [17,18]

$$K = \frac{\pi}{L}\sqrt{4\chi N + 1}. \tag{4}$$

The parameter χ takes values between 0 and 1. A pattern built with $\chi \to 0$ is fully disordered, whereas the choice $\chi \to 1$ leads to a perfect crystal. For details on the numerical procedure to design SHU point patterns, refer to Refs. [24,26].

Let us precisely describe the medium. A SHU point pattern is created at first, with parameter $\chi = 0.6$. We chose this high value in order to increase the minimum distance between two points, allowing us to increase the radius a of the monodisperse set of particles without overlapping and hence to increase the concentration. The ratio $N/L^2 = 3600$ is also kept constant, which induces that the parameter K is constant as well in every plot of the paper. To reach a given concentration $\phi = N\pi a^2/L^2$, the radius a of the particles is modified.

From a propagation point of view, it is well known for years [27] that the intensity scattered by N scatterers is proportional to the structure factor $S(\mathbf{q})$, where $\mathbf{q}$ is the scattering vector $\mathbf{q} = k_0(\mathbf{u}_i - \mathbf{u}_s)$, with ($\mathbf{u}_i$ is the incident wave vector, $\mathbf{u}_s$ is the scattered wave vector, and k_0 is the wave number of the incident field). This relation is only valid in the single scattering regime. From there, in this regime and considering Eq. (2), transparency of SHU media is deduced [17].

For a square domain Ω of size $2K$, transparency window is such that $|\mathbf{q}| < K$ or equivalently $k_0 < K/2$, which can also be written in the form [18]

$$k_0 a \leqslant \sqrt{\pi\phi\chi}. \tag{5}$$

For the sake of legibility, we introduce the reduced wave number $\tilde{k} = 2k_0/K$, such that $0 < \tilde{k} < 1$ is the transparency window of the SHU medium in the single scattering regime. Here, multiple scattering effects are taken into account and are in competition with transparency effects, which are induced by the spatial organization of scatterers.

B. Short-range correlated media: A correlated media with local constraints

In heterogeneous media made of finite-size cylinders, a minimal exclusion distance $b = 2a$ between their centers is naturally imposed by their nonpenetrability. This distance can also be larger but has to be lower than a maximum value imposed by the concentration. For random monodisperse media, the maximum concentration being $\phi_r \approx 83\%$, the upper limit for b is [6]

$$b_{\max} = 2a\sqrt{\frac{\phi_r}{\phi}}. \tag{6}$$

This type of constraints is called SRC because the presence of a cylinder only constraint its neighbourhood, that is to say the position of cylinders located in a circle of radius b around it. For all systems considered in this paper, the minimal exclusion distance $2a$ has to be taken into account in order to avoid overlapping.

The SRC medium is made of cylinders of radius a that cannot overlap. It is understood as an intermediate case between perfectly disordered and SHU media (see Fig. 1 of Ref. [18] and Ref. [6]).

C. Mixing of long- and short-range correlations: Description of the nested medium

In the following, SHU and SRC media are both composed of N particles. The structure factor of the nested medium $S_{\mathrm{Nested}}(\mathbf{q})$ can then be written with respect to the ones of the SRC and SHU media as

$$\begin{aligned} S_{\mathrm{Nested}}(\mathbf{q}) = {} & \frac{1}{2}(S_{\mathrm{SHU}}(\mathbf{q}) + S_{\mathrm{SRC}}(\mathbf{q})) \\ & + \frac{1}{2N}\sum_{m=1}^{N}\sum_{n=1}^{N} e^{-i\mathbf{q}.\mathbf{r}_{\mathbf{m}}^{\mathrm{SHU}}} e^{i\mathbf{q}.\mathbf{r}_{\mathbf{n}}^{\mathrm{SRC}}} \\ & + \frac{1}{2N}\sum_{m=1}^{N}\sum_{n=1}^{N} e^{i\mathbf{q}.\mathbf{r}_{\mathbf{m}}^{\mathrm{SHU}}} e^{-i\mathbf{q}.\mathbf{r}_{\mathbf{n}}^{\mathrm{SRC}}}. \end{aligned} \tag{7}$$

From Eq. (7), we notice that, without coupling between both patterns, the resulting structure factor is directly the average between the two separate structure factors (SRC and SHU).

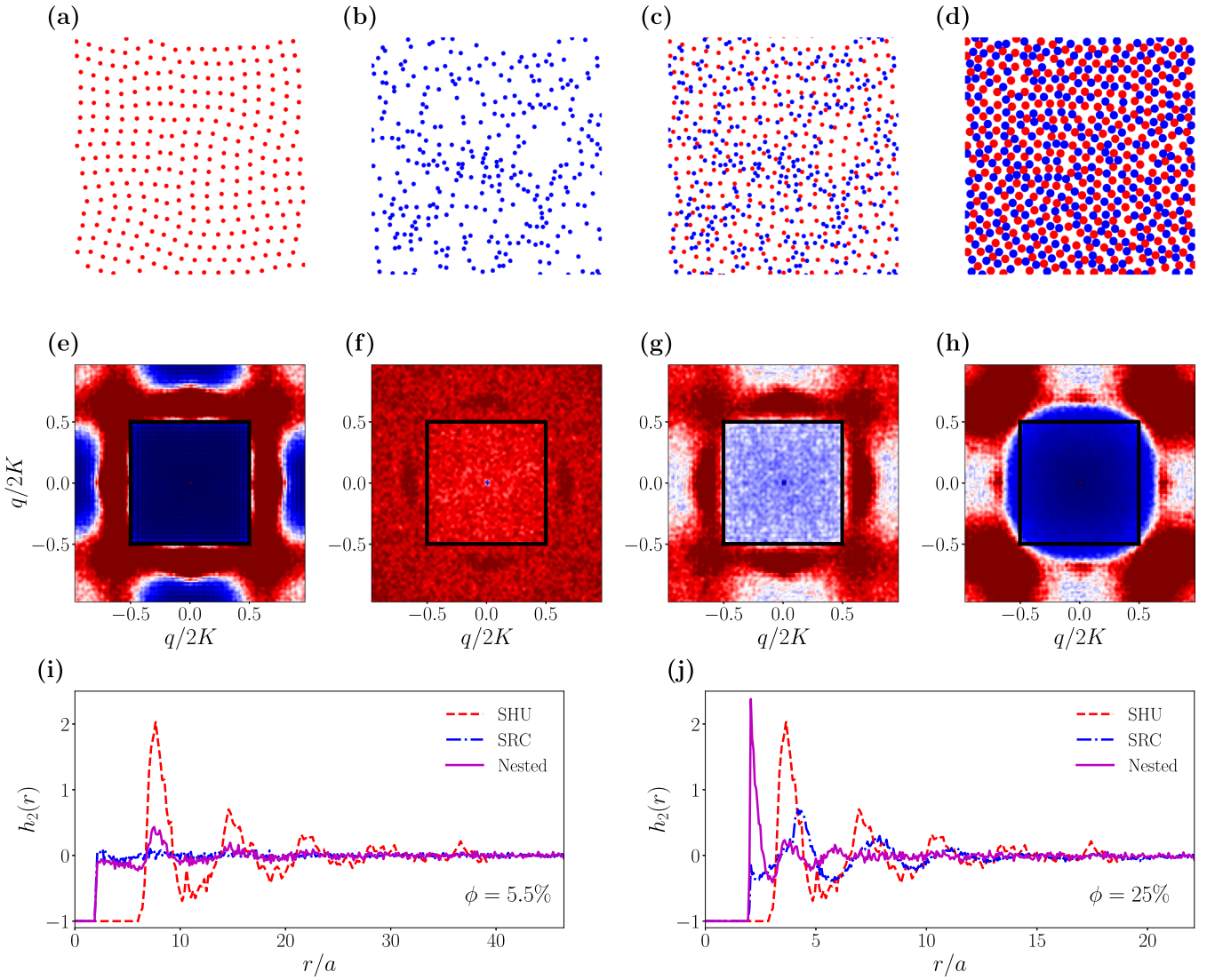


FIG. 1. (a) SHU medium made of cylinders of radius a such that the concentration is $\phi = 5.5\%$; (b) SRC medium with cylinders of same size as (a); (c) nested medium composed of the superposition of media SHU (a) and SRC (b); (d) nested medium made of larger cylinders such that $\phi = 25\%$ and $\phi_{\text{tot}} = 2\phi = 50\%$. (e)–(h) Average structure factors $\langle S(\mathbf{q})\rangle$ respectively of the media (a)–(d). The black square on each plots (e)–(h) corresponds to the domain Ω on which the structure factor $S_{\text{SHU}}(\mathbf{q}) = 0$ (see text). (i) Pair-correlation function of the three media SRC, SHU, and nested for concentration $\phi = 5.5\%$ and (j) same quantities as (i) for $\phi = 25\%$.

This coupling is expected to increase with the size of the particles. Figures 1(a) and 1(e) show a SHU points pattern and its structure factor. Figures 1(b) and 1(f) are the same quantities for an uncorrelated medium, Figures 1(c) and 1(g) for a nested medium whose concentration is $\phi_{\text{tot}} = 2\phi = 11\%$ and the corresponding structure factor averaged over disorder $\langle S(\mathbf{q})\rangle$. In Figs, 1(d) and 1(h) the same quantites are presented for larger particles that lead to $\phi_{\text{tot}} = 2\phi = 50\%$. In this case, the spectral domain Ω is clearly visible, endorsing the fact that the SRC particle pattern is organizing itself, being more constrained by the SHU medium. It must be mentioned that the parameter K is kept constant here, defined with N, the number of cylinders in the SHU medium. Doing so, we keep constant the incident wave number $\tilde{k}$ in every plot of the paper. In Fig. 1(h), the domain where $S(\mathbf{q})$ decreases is larger than $2K$, which endorses the fact that correlations strongly impact the nested medium made of $2N$ particles.

Figures 1(i)–1(j) show the three pair-correlation functions $h_2(r)$ of each medium (SRC, SHU, and nested), for, respectively, $\phi = 5.5\%$ ($\phi_{\text{tot}} = 11\%$) and $\phi = 25\%$ ($\phi_{\text{tot}} = 50\%$). These quantities, computed numerically, allow us to broaden the previous remarks. In Fig. 1(i), no signs of correlation appear for the nested medium except the ones that are already visible on both separated media. This means that, in this case, the coupling between both media is weak. In this case, SRC medium appears to be properly described by the hole correction [$h_2(r) \approx 0\ \forall r > 2a$]. As the concentration increases [see Fig. 1(j)], a strong peak appears around $r = 2a$ in the nested case, which is not visible on SRC and SHU media, showing that this medium is both short- and long-range correlated and that all particles are strongly connected. This strong peak can typically be predicted by analytical methods, such as the one of Percus-Yevick [28,29]. The analysis of the microstructure is more straightforward from $S(\mathbf{q})$ than with $h_2(r)$, in

particular when it comes to analyzing the behavior of SHU. In the following, we will analyze which of these parameters is more accurate to study wave propagation.

III. ANALYSIS OF THE PROPAGATION: LIMITATION OF CLASSICAL APPROACHES

The important point of this paper is to understand the coupling between SRC and SHU media from the point of view of propagation of coherent waves characterized by the effective wave number $k_{\text{eff}} = \omega/c_{\text{eff}} + i\alpha_{\text{eff}}$, with c_{eff} the effective phase velocity and α_{eff} the effective attenuation. This last quantity is linked to the elastic mean-free path by [30]

$$\alpha_{\text{eff}} = 1/2\ell_e \tag{8}$$

since no absorption effects are considered here. In this section, we start by comparing results obtained with the software MuScat [16] and the most common statistical approach for multiple scattering problems, the independent scattering approximation (ISA). The great interest of ISA is to clearly described the propagation of coherent waves in random media provided that the concentration of scatterers is not too large. This model predicts the effective wave number to be

$$k_{\text{ISA}}^2 = k_0^2 - 4in_0 f(0), \tag{9}$$

where $k_0 = \omega/c_0$ is the wave number inside the host medium, ω the pulsation and $n_0 = \phi/\pi a^2$. Here, $f(\theta)$ is the far field form function of a single cylinder, given by

$$f(\theta) = \sum_{n=-\infty}^{+\infty} T_n e^{in\theta}, \tag{10}$$

where the scattering coefficients T_n contain all the elastic properties of the cylindrical elastic particles, that are made of steel (longitudinal wave speed, $c_L = 5700\ \text{ms}^{-1}$, transverse wave speed $c_T = 3000\ \text{ms}^{-1}$, density $\rho_c = 7850\ \text{kgm}^{-3}$) [31]. One important point is that the scattering coefficients T_0 and T_1 of an elastic particle are of the same order of magnitude at low frequency. So, these two modes have always to be considered, but in the extreme case $\phi_{\text{tot}} = 2\phi = 50\%$, for the highest frequencies, the mode $n = 2$ is also needed to reach convergence. In the following, the scattering cross section of a scatterer, required to calculate effective attenuations or elastic mean-free paths, is given by

$$\sigma = \int_0^{2\pi} |f(\theta)|^2 d\theta = \int_0^{2\pi} \sigma_d(\theta) d\theta. \tag{11}$$

The procedure to compute the effective parameters with MuScat is based on the phase difference method and can be found in Refs. [6,16]. Simulations on SRC, SHU, and nested media are performed, averaging over 50 similar disorder realizations for each.

The effective attenuation plotted in Fig. 2 shows that the SHU medium allows the coherent wave to propagate without any loss. This transparency behavior is in perfect agreement with previous results from the literature [17,18]. In this figure, correlation effects are put in light. First, at low concentration, Fig. 2(a) shows that MuScat-SRC (i.e., the MuScat simulations on SRC media) is in agreement with ISA for $\phi = 5.5\%$. This was expected because the SRC medium is almost

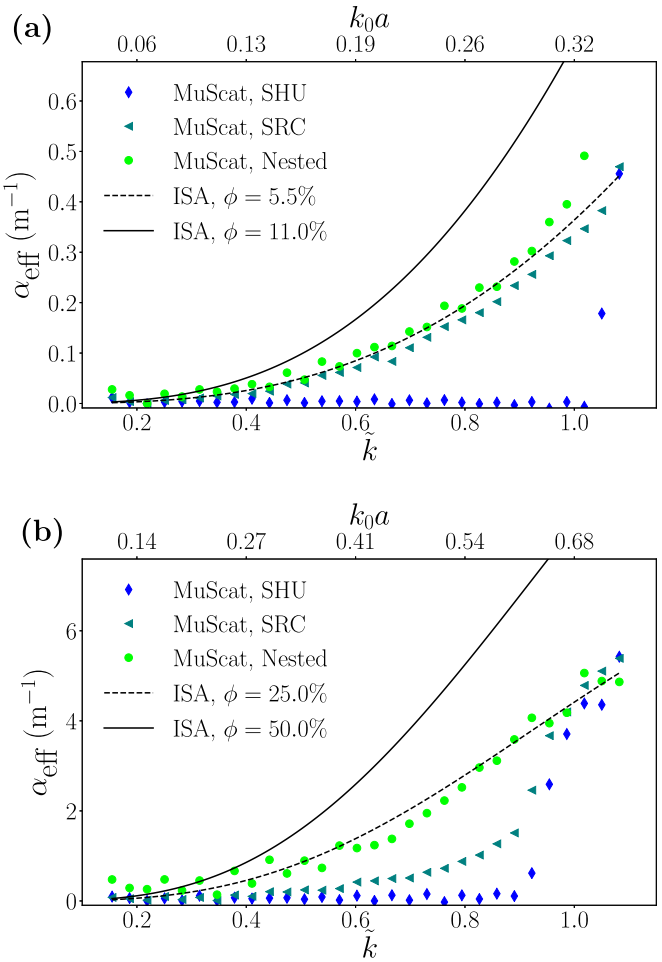


FIG. 2. Effective attenuation calculated with MuScat and with the ISA, for each pattern (SHU, SRC, and nested), for (a) $\phi_{\text{tot}} = 2\phi = 11\%$ and (b) $\phi_{\text{tot}} = 36\%$, with respect to the wave number $\tilde{k} = 2k_0/K$ (see text).

perfectly random for this concentration, and we know that ISA perfectly models the propagation in this case where the correlation does not play any role. Recall that the correlation is a second-order effect. The correlation effects are clearly demonstrated by the MuScat-SHU curve. This one shows the cancellation of the attenuation, which is the signature of acoustic transparency. More interesting, MuScat-nested and ISA curves are very close to each other even if there are correlations in the medium. Here, the nested medium, which is twice as dense as SRC and SHU media, impacts the coherent wave in a very similar way as the SRC medium alone. We can say that the SHU medium is hidden in the SRC medium. Furthermore, this illustrates the weak coupling between the two sets of cylinders when the concentration and the cylinders size are small. However, when considering results in Fig. 2(b), for which the whole concentration is $\phi_{\text{tot}} = 2\phi = 36\%$, the situation is completely different. The MuScat-nested curve no longer matches the MuScat-SRC curve, a strong coupling between SRC and SHU media appears inside the nested medium.

It should also be notice that in Fig. 2(b), the MuScat-SRC curve appears as a transition between the ISA-25%

curve and the MuScat-SHU curve, which enlightens the link between short- and long-range correlations. Increasing distance b inside SRC microstructure makes the wave propagates with less loss, making the medium more transparent than the uncorrelated equivalent medium. The difference between MuScat-nested and MuScat-SRC curves proves that the coupling is here very strong, the result being that the nested medium causes half less loss than the same medium without correlation (ISA-50% curve).

IV. MODEL FOR AVERAGE QUANTITIES

Numerical results extracted with the software MuScat help us understanding the global behavior of the coherent waves that propagate in the different media. However, it does not allow us to distinguish the preponderant effects and the weaker ones, all of them being naturally integrated in the numerical procedure [16]. For this reason, it appears also crucial to make use of statistical models that are built on different restrictive assumptions. These models depend directly on the two quantities $h_2(r)$ and $S(\mathbf{q})$ used to describe the microstructure in Sec. II. We thus have a clear relation between the microstructure and the propagation of the waves. The better agreement of a given approach with MuScat therefore enlighten the relevance of its assumptions, pointing out at the same time the predominance of one physical effect compared to the others. It is noteworthy that the pair-correlation function only involves the relation between two scatterers. The wave propagation models chosen in the following are also of order two in interactions. As the interaction of waves with a scatterer is characterized by the scattering coefficients T_n (eigenvalues of the transition matrix T), the models introduced only use second-order T_nT_m products to characterize the correlation. In this spirit, different models that are essential for the physical analysis are presented briefly in the following.

A. Average field

In this section we briefly present the models we used to describe the propagation of coherent waves. Basically, diagrammatic expansions were introduced in particle physics by Feynmann [32], Dyson [33], and others in order to provide deep physical insight into nature of multiple interactions and correlations between scatterers. The coherent waves result from a statistical averaging over realizations of disorder. Here, let us start directly with the expression of the ensemble average of the Green's function $\langle G\rangle$ verifying the Dyson equation [15,34]

$$\langle G\rangle = \widehat{G} + \widehat{G}\widehat{\Sigma}\langle G\rangle, \tag{12}$$

where $\widehat{\Sigma}$ is the self-energy operator and $\widehat{G}$ is the Green's function that corresponds to the medium either without scatterers or without any correlations between scatterers. Let us define the wave number $\widehat{k}$ inside this medium. Because the medium is assumed to be statistically homogeneous and isotropic, this function is given in Fourier space by $\widehat{G}(k) = (\widehat{k}^2 - k^2)^{-1}$ and $\langle G\rangle$ is consequently of the form

$$\langle G(k)\rangle = \frac{1}{\widehat{k}^2 - k^2 - \widehat{\Sigma}(k)}. \tag{13}$$

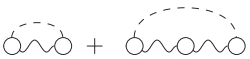
The effective wave number k_{eff} is defined in our case as an eigenvalue of the system, and is solution of

$$k^2 = \widehat{k}^2 - \widehat{\Sigma}(k). \tag{14}$$

The first (and the simplest) approach is to choose the host medium as the reference medium. In that case $\widehat{G} = G_0$ and $\widehat{k} = k_0$ are associated to the homogeneous space without scatterers, we have

$\widehat{\Sigma} = \Sigma =$  (15)

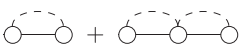
whereas, according to Frisch [15], if $\widehat{G} = \overline{G}$ and $\widehat{k} = \overline{k}$ are associated to the space with uncorrelated scattering events. We get

$\widehat{\Sigma} = \overline{\Sigma} =$  (16)

The impact of the two options (15) and (16) on the dispersive equation will be explained in the following. In these expressions, each circle corresponds to a first-order interaction in the multiple scattering medium associated with the action of the scattering operator T of a single scatterer. The scattering coefficients T_n in Eq. (10) are the eigenvalues of T. The lines between two circles represent the propagation in the reference medium, while the dotted lines represent the correlation between two scattering events. In the following, the formulation (16) is adopted because it allows us to separate concentration effects (adjusting $\overline{k}$) without dealing with correlation effects. The wave number $\overline{k}$ is either replaced by k_{ISA} within the framework of the ISA (first order of interactions), or by k_{LM} within the framework of the QCA (second order of interactions). It is worth noting that effective wave number k_{LM} only models double interactions without correlations between the cylinders positions [35] and is of the form:

$$\overline{k}^2 = k_{\text{LM}}^2 = k_{\text{ISA}}^2 + \frac{8}{\pi k_0^2}\int_0^{\pi} \cot\left(\frac{\theta}{2}\right)\frac{d}{d\theta}[f(\theta)]^2 d\theta. \tag{17}$$

Now that the modeling of $\overline{k}$ has been exposed, the main challenge is to calculate the diagrams of the self-energy operator including pair-correlated scattering events. To do that, we rely on the approach of Fikioris and Waterman (FW), which is based on the QCA (we thus speak about QCA-FW). This approach models the correlation with the pair-correlation function $h_2(r)$. This leads us to the following approximation:

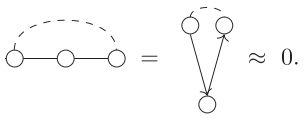
$\overline{\Sigma}_{\text{QCA}} =$  (18)

with the result (cf. Appendix A)

$$k_{\text{eff}}^2 = \overline{k}^2 - 8i\pi n_0^2 \sum_{n,m=-\infty}^{+\infty} T_nT_m \times \int_0^{+\infty} J_{m-n}(k_{\text{eff}}r)H_{m-n}^{(1)}(k_0r)h_2(r)rdr. \tag{19}$$

Two approximations are made to deduce Eq. (18) from Eq. (16). First, diagrams of the same type as the second diagram of Eq. (16) can be neglected under the assumption that

correlations effects are stronger for close pairs of particles. The particle in the middle of the diagram being therefore far from the two others, one can assume diagrammatically



(20)

Second, we assume $T_n(\bar{k}) = T_n(k_0)$ so that the wavy lines of Eq. (16) become straight lines in Eq. (18). Note that $T_n(\bar{k})$ coefficients are involved only in the framework of self-consistent theories as the QCA-CP [36]. Imposing $\bar{k} = k_{\mathrm{ISA}}$ will be denoted FW (ISA), whereas the choice $\bar{k} = k_{\mathrm{LM}}$ will be designated by FW (LM). In the case of monopolar scatterers, it is worth noting that k_{LM} reduces to k_{ISA}. Therefore, Eq. (19) reduces in this case to the well-known expression of Keller's wave number [5,37–39]

$$k_{\mathrm{eff}}^2 = k_{\mathrm{ISA}}^2 - 8i\pi f(0)^2 n_0^2 \times \int_0^{+\infty} J_0(k_{\mathrm{eff}} r) H_0^{(1)}(k_0 r) h_2(r) r dr. \tag{21}$$

B. Average intensity

To calculate the scattering mean-free path $\ell_e = 1/2\alpha_{\mathrm{eff}}$, another way consists in analyzing the average intensity, driven by the Bethe-Salpeter equation. In this framework, it is efficient to introduce the average structure factor $\langle S(\mathbf{q})\rangle$, which is calculated by ensemble averaging Eq. (1). The structure factor is intrinsically linked to $h_2(r)$ and provides another point of view to analyze the behavior of the microstructure of multiscattering media.

This quantity, for cylinders located on a surface $\mathscr{S}$, can be written as

$$\langle S(\mathbf{q})\rangle = 1 + \frac{N-1}{\mathscr{S}^2} \iint_{\mathscr{S}^2} [1 + h_2(r_{jk})] e^{j\mathbf{q}\cdot(\mathbf{r}_j - \mathbf{r}_k)} d\mathbf{r}_j d\mathbf{r}_k. \tag{22}$$

Then, by definition of the Fourier transform and noting $|\Theta(\mathbf{q})|^2 = \iint_{\mathscr{S}^2} e^{j\mathbf{q}\cdot(\mathbf{r}_j - \mathbf{r}_k)} d\mathbf{r}_j d\mathbf{r}_k$ the spatial Fourier transform of the surface $\mathscr{S}$, we get [17]

$$\langle S(\mathbf{q})\rangle = 1 + \frac{N-1}{\mathscr{S}} \widetilde{h}_2(\mathbf{q}) + \frac{N-1}{\mathscr{S}^2} |\Theta(\mathbf{q})|^2, \tag{23}$$

where $\widetilde{h}_2(|\mathbf{q}|)$ is the Fourier transform of $h_2(r)$, used in Dyson approaches described just before. If the finite-size effects caused by $\Theta(\mathbf{q})$ are eliminated, a corrected structure factor $\langle S_{\mathrm{corr}}(\mathbf{q})\rangle = \langle S(\mathbf{q})\rangle - \frac{N-1}{\mathscr{S}^2}|\Theta(\mathbf{q})|^2$ can be introduced leading to the expression of the effective attenuation [26,27,40,41]

$$\frac{1}{2\ell_e} = \alpha_{\mathrm{HF}} = \frac{n_0 \sigma}{4\pi} \int_\Omega \langle S_{\mathrm{corr}}[k_r(\mathbf{u} - \mathbf{u}')]\rangle d\Omega, \tag{24}$$

with σ given by Eq. (11) and $k_r = \mathrm{Re}(\sqrt{k_{\mathrm{eff}}^2})$ [17]. Relation (24) is derived in the context of punctual scatterers. It is consistent with earlier works. Among them, Ref. [41] appears to be one of the first to prove its validity through comparison with experiments. However, Hart and Farrell already used it in their work on the cornea [27]. This is the reason why we denote "HF" the predictions based on Eq. (24). Furthermore, one common way to take anisotropic effects into account is to use the interference approximation (ITA) that leads to write the correction [5,7]:

$$\frac{1}{2\ell_e} = \alpha_{\mathrm{ITA}} = \frac{n_0}{4\pi} \int_\Omega \sigma_d[\arg(\mathbf{u} - \mathbf{u}')] \langle S_{\mathrm{corr}}[k_r(\mathbf{u} - \mathbf{u}')]\rangle d\Omega. \tag{25}$$

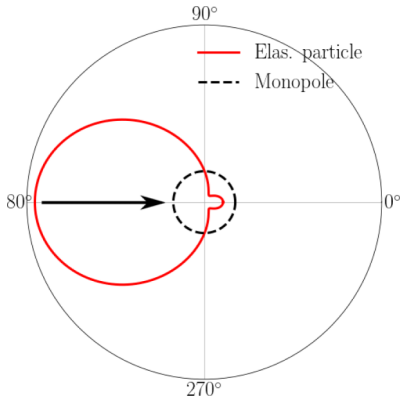


FIG. 3. Differential scattering cross section σ_d calculated for an elastic particle and a monopolar scatterer, for a frequency such that $k_0 a = 0.25$.

V. PROPAGATION OF THE COHERENT WAVE IN SHORT- AND LONG-RANGE CORRELATED MEDIA

A. Importance of the anisotropic scattering of elastic particles on the coherent waves

The QCA-FW, dealing with the pair-correlation function, allows to consider scatterers with angular radiation patterns leading to scattering cross sections containing several modes of vibration. Even at very low frequency, the two first vibration modes are necessary in order to describe scattering cross sections, which leads to anisotropic scattering cross section, as shown in Fig. 3. Two simulations are presented in Fig. 4 showing that this point is essential in the calculation of the correlation. In the first case, purely monopolar (isotropic) scattering is considered by numerically canceling the dipolar mode. In this case, it is worth noting that Keller's predictions agree with HF's predictions for $\tilde{k} < 1$, which means that the SHU transparency nature of the medium is caught. In the second case, where real elastic particles are considered, Keller's model fails to estimate the effective attenuation. As shown by MuScat results, transparency remains but calculating k_{eff} with Eq. (21) does not succeed in predicting it. This is the reason why the QCA-FW is introduced and adopted in the following.

An important contribution of this section is to show that the models FW (ISA) and FW (LM) lead to a very good prediction of the wave numbers for all the microstructures, SRC, SHU, and nested. This is a result, which has already been established for dense random media, where the Percus-Yevick approximation is generally used [42], but which is original for SHU and nested media. In the following, the FW (ISA) model is shown to account for spatial correlations in the cases where the cylinders radii are relatively small. This is the most common situation encountered in the literature. At higher concentrations, when multiple scattering effects increase, we

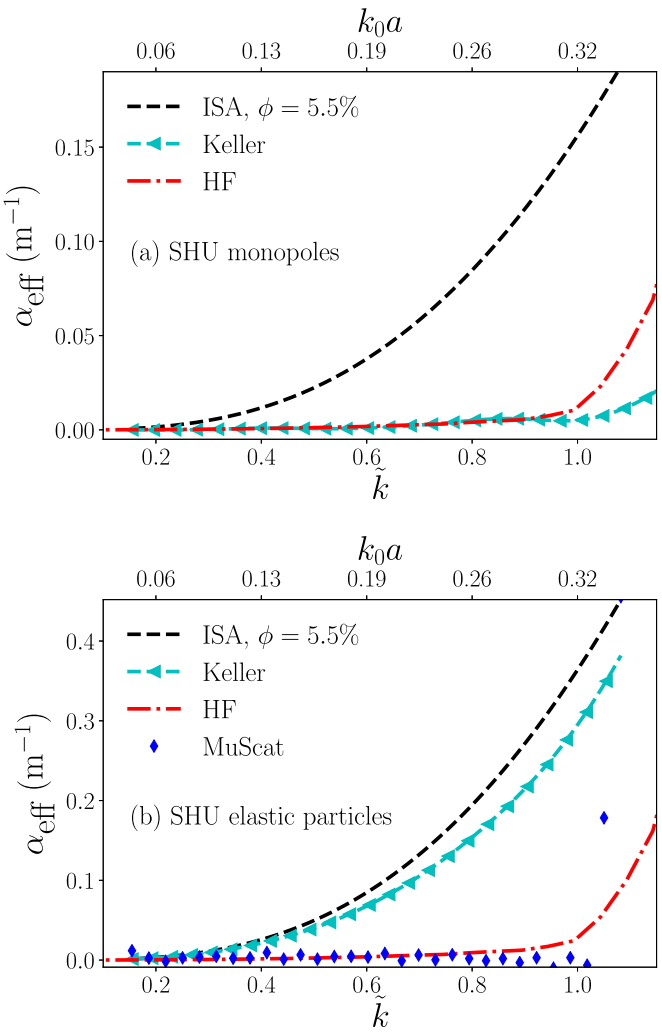


FIG. 4. Effective attenuation in the SHU medium comparison between MuScat, Keller, and HF approaches. Concentration $\phi = 5.5\%$.

show that the use of FW (LM) improves the predictions of FW (ISA). This result can be easily understood because the k_{LM} wave number is of the second order in concentration unlike k_{ISA}, which is of the first order.

B. Modelling of the correlation in dilute media

In Fig. 5(a), we clearly see that FW (ISA) perfectly captures the SHU transparency properties of the medium. It validates the fact that the pair-correlation function $h_2(r)$ properly describes the microstructure of a SHU medium, as already observed in a recent study [43] that deals with pointlike particles. Furthermore, the use of the function $h_2(r)$ is relevant to model the propagation inside the media, endorsing the fact that pair interactions are predominant.

Let us now analyze statistical predictions based on the average intensity. For the first particles size [Figs. 5(a)–5(c)] the concentration is $\phi_{\text{tot}} = 2\phi = 11\%$, allowing the assumption $k_r \approx k_0$ for the calculation of ℓ_e with Eq. (24). It is worth noting that FW (ISA) and HF predictions give very close results for each case (SHU, SRC, and nested). The physical interpretation is clear: even if diagrammatic expansions are truncated to interactions of order two, the Ward identity, which expresses the conservation of energy, is still verified in a good approximation. Rigorously speaking, recurrent scattering has also to be taken into account as well, which is negligible for not too dense systems out of resonance. It is worth noting in Fig. 5(c) that FW (ISA) and HF slightly underestimate the effective attenuation given by MuScat, proving that the densification of the medium has a strong influence on the coherent wave propagation.

A strong advantage of the model based on the mean field (FW) is that it provides a full expression of the entire wave number. This allows to examine the effective phase velocity, much more difficult to extract through the intensity. In Fig. 6, we plot this quantity, calculated for the three sets of particles. This choice is motivated by the fact that in this case the effect of correlations strongly appear for the highest frequencies, even at low concentration ($\phi = 5.5\%$). The agreement is quantitative between FW (ISA) and MuScat, endorsing the fact that correlations also impact the phase velocity, near the transition frequency $\tilde{k} = 1$. As opposed to the attenuation results [Fig. 2(a)], the presence of the SHU particles modifies the phase velocity. This results could appear useful for interesting applications such as wave guiding [44].

C. Effective wave numbers in dense correlated media

Overall, all the models except that of Keller agree among themselves for the diluted media. But what happens when the concentration and multiple scattering effects increase?

This leads to consider now $\phi = 18\%$ for each sets of particles (the nested medium has then a concentration of $\phi_{\text{tot}} = 36\%$). This leads at the same time to an increase of the coupling between the two populations: the SHU cylinders constraint more the SRC ones, which have less place to fit between the SHU cylinders. Also, the product k_0a is increasing proportionally. To adjust the two different approaches (FW and HF), FW (LM) is considered instead of FW (ISA), and α_{ITA} [Eq. (25)] is also computed.

In Figs. 5(d)–5(f), the effective attenuations of the three media are presented. For the SHU medium, we see that all the models are in good agreement with MuScat, even if FW (LM) predicts an increase for the high-frequency range. For the SRC medium, an important difference is visible between FW (LM) and MuScat on one side and FW (ISA), HF and the ITA on the other side. It should be pointed out that ITA only rectifies HF significantly for the highest frequencies, and that the correction is the opposite of what is expected, making the medium less opaque. This tendency was already pointed out by Derode *et al.* on SRC media [5], demonstrating that ITA does not improve HF to model the propagation in this case. On the other hand, FW (LM) is very close to MuScat, which shows the efficiency of the correction provided by adjusting $\overline{k} = k_{\text{LM}}$ in Eq. (19). This efficiency is even more visible in the results for the nested medium in Fig. 5(c). Curiously, taking into account the angular radiation of the scatterers improves the FW model but not the HS ones resulting from the average intensity approach.

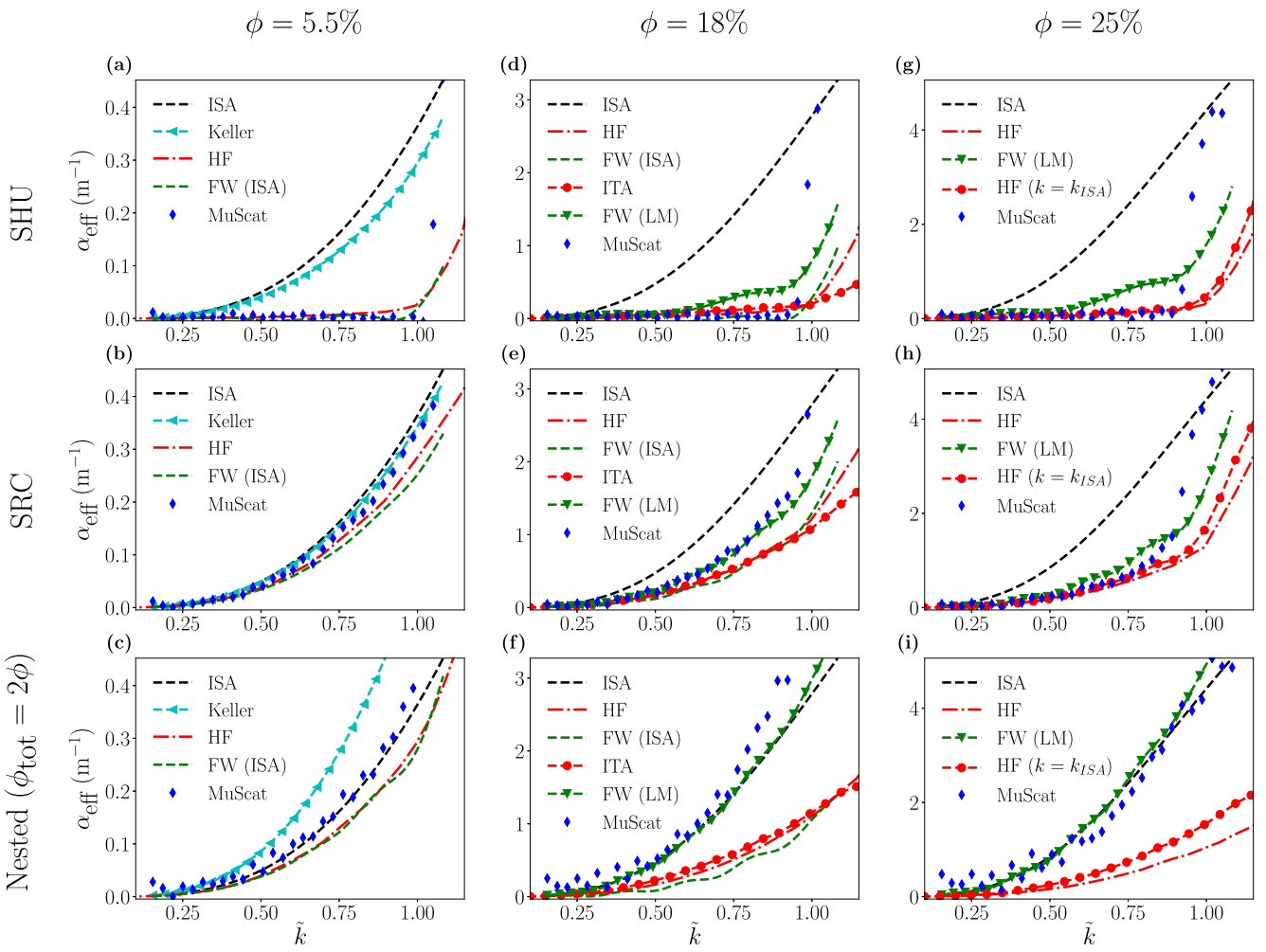


FIG. 5. Effective attenuation calculated with different approaches for the different media (SHU, SRC, and nested) presented in Fig. 1. The concentration ϕ of SRC and SHU media is controlled by the radius a of the particles (see text). The frequency window is kept constant such that $k_0 a \in [0.05 - 0.35]$ for $\phi = 5.5\%$ (a)–(c), $k_0 a \in [0.09 - 0.63]$ for $\phi = 18\%$ (d)–(f), $k_0 a \in [0.1 - 0.735]$ for $\phi = 25\%$ (g)–(i).

Here, we see that the FW (ISA) and FW (LM) models, where the correlation is calculated from $h_2(r)$, are more relevant than the HF model, which is directly related to the structure factor, cf. Eqs. (24).

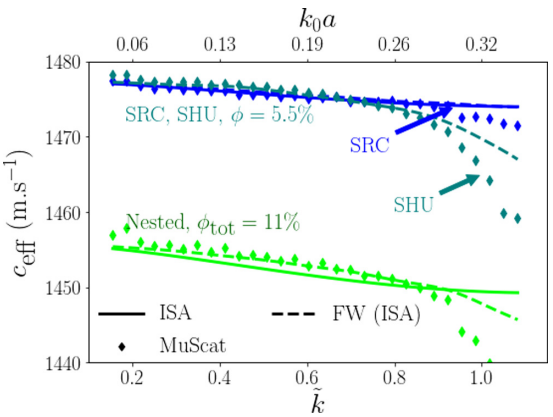


FIG. 6. Effective phase velocity in a SHU medium for which $\phi = 5.5\%$.

What happens when the particles size increases, as much as $\phi_{tot} = 50\%$? It could appear justified to contest the previous assumption $k_r \approx k_0$. A simple way to rectify this assumption is to set $k_r = k_{ISA}$. This leads to consider the background medium as a uncorrelated medium, already homogenized. It is worth noting in Fig. 5(g)–5(i) that the corrections are too weak. Other numerical test have been performed with k_{LM} instead of k_{ISA} without improving our results. So, other higher diagrams appear to be necessary to properly describe the effective attenuation with the HF approach. In our recent study [18], it was demonstrated that adding higher-order diagrams properly corrected the attenuation in the case of a SHU medium. Indeed, these diagrams lead to a correction in attenuation of approximately $2\alpha_{ISA}^2/k_0$ (order of magnitude) [17]. For our nonresonant system, these diagrams of third order in interactions are to be taken account before recurrent scattering. Here, the discussions about higher-order terms would have taken us to far, and therefore is out of the scope of this paper. Together, results of Fig. 5 allow us to confirm that the model FW(LM) is the most robust against correlation and concentration effects.

VI. CONCLUSION

Our study deals with different types of microstructures: SRC, SHU, and nested. The two first have been considered in the recent past, the effective properties of nested media are presented here.

The concentration in the different media is driven by the radius of the cylinders. Increasing this quantity leads at the same time to an increase of the concentration and to the self-organization of the multiple scattering medium: the SHU particles constraint more and more the SRC ones, which have less place to fit between the SHU cylinders. If, for small cylinders, SRC medium can be assimilated to an uncorrelated one, the short-range correlations increase with the concentration. Finally, the nested medium, composed of the SHU and SRC media, exhibits both short- and long-range correlations.

Interestingly, whatever the concentration and the degree of interaction between the particles, the nested medium, which is twice as dense as SRC and SHU media, impacts the attenuation of coherent waves in the exact same way as an uncorrelated medium with half of particles. In other words, we can say that half of the particles of the nested medium are invisible, even at very large concentration. However, the presence of the SHU particles in the nested medium notably modifies the phase velocity. So inserting a SHU in a random medium can change the velocity without changing the attenuation. These results could appear useful for interesting applications such as wave guiding or focusing.

Two models derived from the QCA, FW (ISA), and FW (LM), have been developed within the framework of diagrammatic expansions and the Dyson equation in order to calculate the effective wave numbers. These models depend directly on the pair-correlation function $h_2(r)$ introduced to describe the microstructures. With the idea of establishing a link between the microstructure and the wave propagation, we have also used a model derived from the Bethe-Salpeter equation, which describes the imaginary part of the effective wave number with regard to the structure factor. The two quantities $h_2(r)$ and $S(\mathbf{q})$ have the main interest to describe both the microstructure and to represent the correlation in the expression of the effective wave number. We thus have a clear relation between the microstructure and the propagation of the waves.

At low concentration, multiple scattering effects are minimized, and all the models used lead to the same results, except that of Keller [5,15,39], which is the most used for years. We showed that the Keller's model fails because it does not take into account the anisotropic radiation of the particles in the calculation of the correlation.

An important issue of the paper is to show that the models FW (ISA) and FW (LM) lead to very good calculations of the wave numbers for all the microstructures, SRC, SHU, and nested. Hence, second-order interactions are enough to properly describe the propagation in our systems, even if the correlation is long range, the particles large and the multiple scattering strong. If these kinds of results are known for dense random media, where the Percus-Yevick approximation is generally used [42], it is original for SHU, SRC, and nested media when the microstructure is far more complex.

ACKNOWLEDGMENTS

This research is supported by LABEX WIFI (Laboratory of Excellence within the French Program "Investments for the Future") under references ANR-10-LABX-24 and ANR-10-IDEX-0001-02 PSL*.

APPENDIX: THEORY OF FIKIORIS AND WATERMAN

Here, we use the theory of Fikioris and Waterman [45] as the basis of our developments to take into account the correlation. We could thus speak of QCA-FW.

The basic idea developed by Fikioris and Waterman [45] is to project the fields on the cylindrical harmonics. Let A_n be the unknown coefficients resulting from the projection, one finds that k_{eff} and the unknown coefficients A_n are linked by the Lorentz-Lorenz law

$$A_n + \frac{2\pi n_0}{k_0^2 - k_{\text{eff}}^2} \sum_{p=-\infty}^{+\infty} T_p A_p \mathscr{N}_{n-p}(k_{\text{eff}} b) = 0, \tag{A1}$$

where

$$\mathscr{N}_p(k_{\text{eff}} b) = N_p(k_{\text{eff}} b) + \left[\frac{k_{\text{eff}}^2}{k_0^2} - 1\right] M_p(k_{\text{eff}}, b) \tag{A2}$$

and

$$N_p(k_{\text{eff}} b) = (k_{\text{eff}} b) J_p'(k_{\text{eff}} b) H_p^{(1)}(k_0 b) - k_0 b J_p(k_{\text{eff}} b) H_p'^{(1)}(k_0 b), \tag{A3a}$$

$$M_p(k_{\text{eff}}, b) = \int_b^{+\infty} H_p^{(1)}(k_0 r) J_p(k_{\text{eff}} r) h_2(r) k_0^2 r dr. \tag{A3b}$$

The hole correction consists in setting $b = 2a$ to avoid the scatterers from overlapping. Eq. (A1) is a homogeneous linear system of equations

$$\left\{ I + \frac{2\pi n_0}{k_0^2 - k_{\text{eff}}^2} \mathscr{N} T \right\} . \mathbf{A} = 0, \tag{A4}$$

where $\mathbf{A}$ contains the modal amplitudes A_n, I is the identity matrix, T the matrix with coefficient $T_{nm} = T_n \delta_{nm}$ and

$$\mathscr{N}(k_{\text{eff}} b) = N_p(k_{\text{eff}} b) + \left(\frac{k_{\text{eff}}^2}{k_0^2} - 1\right). \tag{A5}$$

Canceling the determinant of the matrix of this infinite system of equations (A4) yields the desired dispersion relation for k_{eff}. Here we use cumulative development, which allows us to write the determinant of any matrix X as a sum

$$\det(I + X) = \sum_{n=0}^{+\infty} Q_n(X), \tag{A6}$$

where operators Q_n are defined by recurrence

$$Q_0 = 1,$$

$$Q_n(X) = \frac{1}{n} \sum_{p=1}^{n} (-1)^{p+1} Q_{n+p}(X) \text{tr}(X^p). \tag{A7}$$

The originality and the main interest of this method is to offer a direct way to select how many orders of interactions are taken into account, without any *a priori*

consideration on concentration values. Q_1 describes the interaction with one particle, Q_2 with two particles and so on. Hence, truncating Eq. (A6) to second order follows the same idea that the one used in order to approximate the self-energy operator in the Dyson equation. Doing so, we find that

$$1+\frac{2\pi n_0}{k_0^2-k_{\rm eff}^2}\mathscr{N}_0(k_{\rm eff}b)f(0)+\frac{1}{2}\left(\frac{2\pi n_0}{k_0^2-k_{\rm eff}^2}\right)^2\mathscr{N}_0(k_{\rm eff}b)^2f(0)^2-\frac{1}{2}\left(\frac{2\pi n_0}{k_0^2-k_{\rm eff}^2}\right)^2\sum_n\sum_k T_kT_n[\mathscr{N}_{n-k}(k_{\rm eff}b)]^2=0. \tag{A8}$$

QCA-FW effective wave number takes the following form [45,46]:

$$k_{\rm FW}^2=k_{\rm ISA}^2+\left(d_2^{\rm conc}+d_2^{\rm corr}\right)n_0^2, \tag{A9}$$

where

$$d_2^{\rm conc}=\frac{-4i\pi}{k_0^2}\sum_{n,m=-\infty}^{+\infty}T_nT_m\left\{\left[k_0^2b^2-(m-n)^2\right]J_{m-n}(k_0b)H_{m-n}^{(1)}(k_0b)-k_0^2b^2J'_{m-n}(k_0b)H_{m-n}^{\prime(1)}(k_0b)\right\} \tag{A10}$$

and

$$d_2^{\rm corr}=-8i\pi\sum_{n,m=-\infty}^{+\infty}T_nT_m\int_b^{+\infty}J_{m-n}(k_{\rm FW}r)H_{m-n}^{(1)}(k_0r)h_2(r)rdr. \tag{A11}$$

For the low-frequency regime where only modes $n=0$ and $n=1$ are needed, no integral divergence appears in the integral equation the governs the effective mean fields, which makes useless the introduction of the radius of exclusion b in the model. Therefore, as in Ref. [35], we can assume that $b\to 0$ in the previous equations.

In this limit, the term $d_2^{\rm conc}$ does not contain any microstructure information and becomes equal to the second-order term of the model derived by Linton and Martin [35], namely

$$\lim_{b\to 0}d_2^{\rm conc}=\frac{8}{\pi k_0^2}\int_0^{\pi}\cot\left(\frac{\theta}{2}\right)\frac{d}{d\theta}[f(\theta)]^2d\theta. \tag{A12}$$

Finally, we find the expression (19) that we use to tackle the physical problems of the paper.

[1] Z. Q. Zhang, I. P. Jones, H. P. Schriemer, J. H. Page, D. A. Weitz, and P. Sheng, Phys. Rev. E **60**, 4843 (1999).
[2] A. Derode, A. Tourin, and M. Fink, Phys. Rev. E **64**, 036605 (2001).
[3] L. L. Foldy, Phys. Rev. **67**, 107 (1945).
[4] M. Lax, Phys. Rev. **85**, 621 (1952).
[5] A. Derode, V. Mamou, and A. Tourin, Phys. Rev. E **74**, 036606 (2006).
[6] A. Rohfritsch, J.-M. Conoir, T. Valier-Brasier, and R. Marchiano, Phys. Rev. E **101**, 023001 (2020).
[7] K. Vynck, R. Pierrat, R. Carminati, L. S. Froufe-Pérez, F. Scheffold, R. Sapienza, S. Vignolini, and J. J. Sáaenz, arXiv:2106.13892 [physics.optics].
[8] Y. Jiao, T. Lau, H. Hatzikirou, M. Meyer-Hermann, J. C. Corbo, and S. Torquato, Phys. Rev. E **89**, 022721 (2014).
[9] K. M. Meek and C. Knupp, Prog Retin Eye Res. **49**, 1 (2015).
[10] N. W. Ashcroft and J. Lekner, Phys. Rev. **145**, 83 (1966).
[11] K. Vynck, R. Pierrat, and R. Carminati, Phys. Rev. A **94**, 033851 (2016).
[12] B. X. Wang and C. Y. Zhao, J. Opt. Soc. Am. B **37**, 1757 (2020).
[13] S. Torquato, Phys. Rep. **745**, 1 (2018).
[14] S. Torquato, G. Zhang, and F. H. Stillinger, Phys. Rev. X **5**, 021020 (2015).
[15] U. Frisch, *Probabilistic Methods in Applied Mathematics*, edited by A. T. Bharucha-Reid (Academic Press, New York, 1968), Vol. 1.
[16] A. Rohfritsch, J-M. Conoir, R. Marchiano, and T. Valier-Brasier, J. Acoust. Soc. Am. **145**, 3320 (2019).
[17] O. Leseur, R. Pierrat, and R. Carminati, Optica **3**, 763 (2016).
[18] A. Rohfritsch, J.-M. Conoir, T. Valier-Brasier, and R. Marchiano, Phys. Rev. E **102**, 053001 (2020).
[19] G. J. Aubry, L. S. Froufe-Pérez, U. Kuhl, O. Legrand, F. Scheffold, and F. Mortessagne, Phys. Rev. Lett. **125**, 127402 (2020).
[20] V. Romero-García, N. Lamothe, G. Theocharis, O. Richoux, and L. M. García-Raffi, Phys. Rev. Appl. **11**, 054076 (2019).
[21] S. Kuznetsova, J. P. Groby, L. M. Garcia-Raffi, and V. Romero-García, Waves Random Complex Media (2021), doi: 10.1080/17455030.2021.1948630.
[22] A. Gabrielli, M. Joyce, and F. S. Labini, Phys. Rev. D **65**, 083523 (2002).
[23] S. Torquato and F. H. Stillinger, Phys. Rev. E **68**, 041113 (2003).
[24] O. U. Uche, F. H. Stillinger, and S. Torquato, Phys. Rev. E **70**, 046122 (2004).
[25] O. U. Uche, S. Torquato, and F. H. Stillinger, Phys. Rev. E **74**, 031104 (2006).
[26] O. Leseur, Ph.D. thesis, Université Pierre et Marie Curie, 2016.
[27] R. W. Hart and R. A. Farrell, J. Opt. Soc. Am. **59**, 766 (1969).
[28] J. K. Percus and G. J. Yevick, Phys. Rev. **110**, 1 (1958).
[29] F. Mandel, J. Chem. Phys. **62**, 1595 (1975).

[30] A. Lagendijk and B. A. van Tiggelen, Phys. Rep. **270**, 143 (1996).
[31] J. J. Faran, J. Acoust. Soc. Am. **23**, 405 (1951).
[32] R. P. Feyman, Phys. Rev. **76**, 749 (1949).
[33] F. J. Dyson, Phys. Rev. **75**, 1736 (1949).
[34] I. Baydoun, D. Baresch, R. Pierrat, and A. Derode, Phys. Rev. E **94**, 053005 (2016).
[35] C. M. Linton and P. A. Martin, J. Acoust. Soc. Am. **6**, 3413 (2005).
[36] L. Tsang and J. A. Kong, *Scattering of Electromagnetic Waves: Advanced Topics* (Wiley, New York, 1995).
[37] F. C. Karal and J. B. Keller, J. Math. Phys. **5**, 537 (1964).
[38] J. B. Keller, *Proceedings of Symposia in Applied Mathematics*, edited by R. Bellman (American Mathematical Society, Providence, 1964), Vol. 16, pp. 145–170.
[39] S. Durant, O. Calvo-Perez, N. Vukadinovic, and J.-J. Greffet, J. Opt. Soc. Am. A **24**, 2943 (2007).
[40] G. Maret and P. E. Wolf, Z. Phys. B: Condens. Matter **65**, 409 (1987).
[41] S. Fraden and G. Maret, Phys. Rev. Lett. **65**, 512 (1990).
[42] M. Caleap, B. W. Drinkwater, and P. D. Wilcox, J. Acoust. Soc. Am. **131**, 2036 (2012).
[43] J. Kim and S. Torquato, New J. Phys. **22**, 123050 (2020).
[44] G. Gkantzounis, T. Amoah, and M. Florescu, Phys. Rev. B **95**, 094120 (2017).
[45] J. G. Fikioris and P. C. Waterman, J. Math. Phys. **5**, 1413 (1964).
[46] A. N. Norris and J.-M. Conoir, J. Acoust. Soc. Am. **129**, 104 (2011).